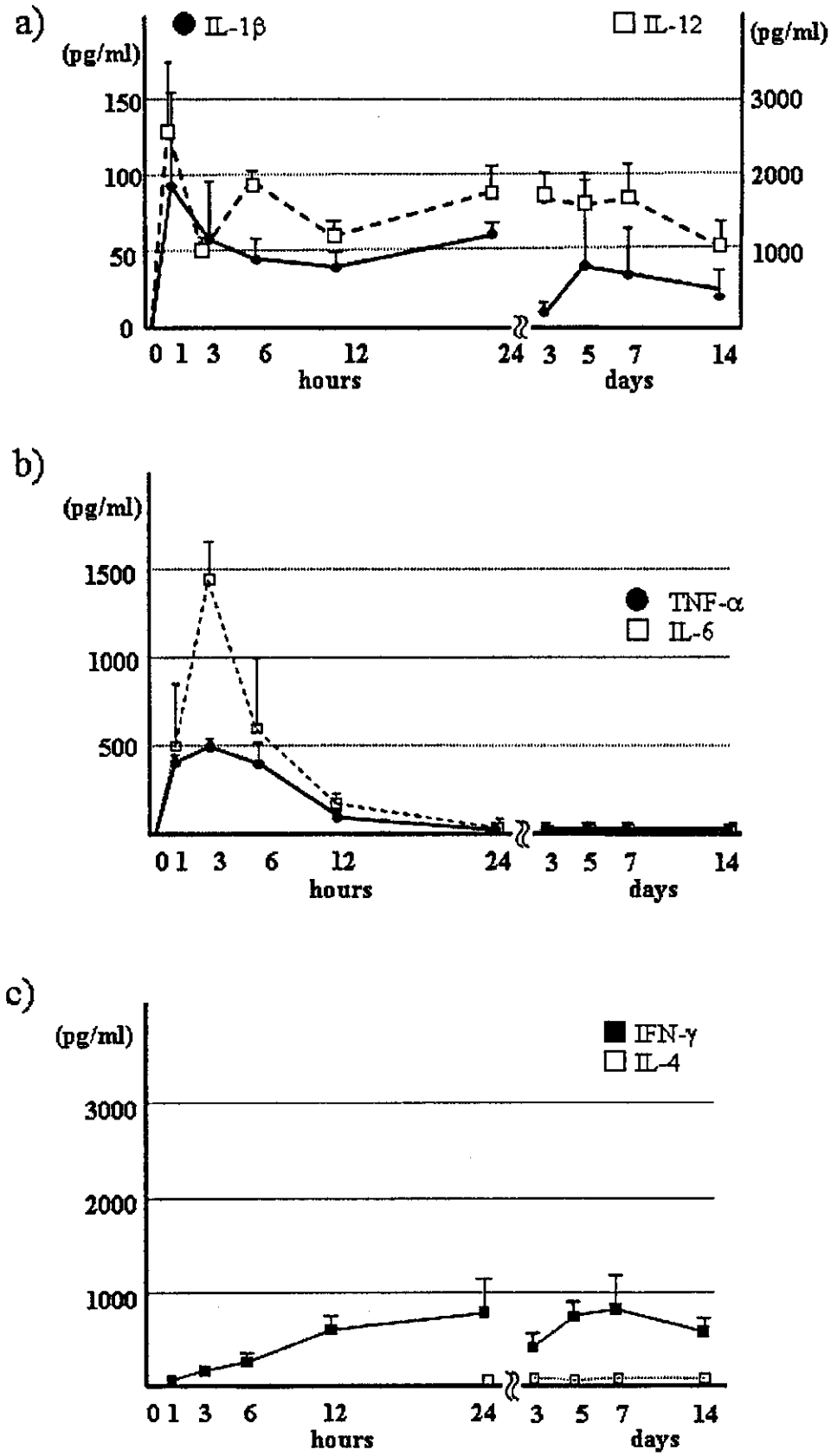

Fig. 3. Time course of serum cytokines after intraperitoneal injection of CADS. (a) Time course of serum IL-1β and IL-12 after injection of CADS, (b) time course of serum TNF-α and IL-6 after injection of CADS, (c) time course of serum IFN-γ and IL-4 after injection of CADS.

discussed the role of inflammatory cytokines in patients with a genetic predisposition to developing coronary arteritis (7, 8). The animal model is considered to be very useful for clarifying the pathogenesis of arteritis in these patients and may allow for the identification of specific treatments for the disease. With the observed differences in the incidence of arteritis in C3H/HeN mice and CBA/JN mice, it can be derived that genetic differences of the mouse strains does influence arteritis. Therefore, it was considered that C3H/HeN may express or attenuate the expression of genes that govern the susceptibility to coronary arteritis.

In the present study, we showed that the loci governing suggestive susceptibility to coronary arteritis were situated on chromosome 1 even though possibility on other chromosome loci may exist. Two of 11 markers on chromosome 1, *D1Mit171* and *D1Mit245* (map position 20.2 cM), appeared to be involved in the susceptibility loci to the development of coronary arteritis. This chromosomal region influences the IL-1 receptors types 1 and 2 (*Il1r1* and *Il1r2*, 19.5 cM). In addition, our results here revealed that IL-1β in sera rapidly increased after intraperitoneal injection of CADS. These findings suggest a ligand-receptor interaction between IL-1β and the IL-1 receptor, which may affect the onset of arteritis. It has been reported that IL-1β regulates vascular damage *in vitro*. Specifically, IL-1β directly injures endothelial cells; however, mechanisms of endothelial cell injury are unclear. Interestingly, an indirect role of IL-1β in the regulation of neutrophil-mediated killing of endothelial cells has been reported (3, 4, 12, 18). Adhesive interaction between activated neutrophils and endothelial cells was facilitated by exposure to IL-1β and superoxide anion, produced by activated neutrophils, and subsequently damaged neighboring endothelial cells (1).

One of the peculiar histological features of arteritis in this model was the severe neutrophilic infiltration observed in the afflicted artery, suggesting an important role of neutrophil activation in the development of arteritis. In addition, it has been reported that the specific antigen to autoantibodies, myeloperoxidase-anti-neutrophil cytoplasmic antibody (MPO-ANCA), targeting its antigen MPO were closely related to the development of coronary arteritis using MPO-deficient mice (17). It is considered that coronary arteritis in this model must be genetically regulated by interactions between neutrophils and endothelial cells modulated by IL-1β. Furthermore, the allelic polymorphism of both *Il1r1* and *Il1r2* and the functional relevance of their polymorphism may be a necessity.

On the other hand, *D4Mit285* (map position 71.0 cM) on chromosome 4 showed negative effect against affectability to coronary arteritis, however this marker showed a probability of 0.017. Several genes related to inflammation are coded around *D4Mit285* on chromosome 4, including TNF receptor superfamily member 1b, 8, and 9 (*Tnfrsf1b*, *Tnfrsf8*, and *Tnfrsf9*) (75.5 cM). The functional relevance of this is seen with the rapid increase of TNF-α following elevation of IL-1β after exposure to CADS. There are also studies that claim IL-1β and TNF-α can induce endothelial cell injury by activated neutrophils (3, 4, 12, 18). Therefore, some of these genes are considered to be protective against the development of coronary arteritis, even in the susceptible C3H/HeN strain. However, the marker *D2Mit265* (χ^2=3.61, P=0.058) on chromosome 2, on which IL-1β is located, did not indicate a significant difference. Th-1 cytokines, such as IL-12 and IFN-γ were also produced by exposure of CADS. It was considered that Th-1 type immunity might have an influence on the development of arteritis in this model; however, we have no direct evidence in the present study to determine whether or not the genes of these cytokines affected the coronary arteritis outcome, since the number of microsatellite markers was insufficient to examine these genomic regions.

The difference in the incidence of coronary arteritis between C3H/HeN and CBA/JN may be attributed to differences in the regulation of genes encoding inflammatory cytokines. It may be concluded from the present study that the development of coronary arteritis is multi-factorial and controlled with cumulative effects of these multiple gene loci in this mouse model.

The authors thank Ms. Hitomi Yamada for her technical assistance and, Drs. Kei Takahashi in Toho University Medical School, Akiko Okawara in National Institute of Infectious Diseases and Masato Nose in Ehime University Medical for their helpful discussion in this work. This study was supported in part by Project Research Grants No. 11-26, 12-30, and 13-19 from the Toho University School of Medicine, Ministry of Education, Culture, Sports, Science and Technology for KT and KS, Ministry of Health, Labour and Welfare for KT and KS, Japan Health Science Foundation for KS, and a research fellowship from the Japan Society for the Promotion of Science for ASP. All experiments described in this study were performed in accordance with the current laws of Toho University and National Institute of Infectious Diseases in Japan.

References

1) Alex, B.L., and Peter, A.W. 2000. Regulation of inflammatory vascular damage. J. Pathol. **190**: 343–348.
2) Atobe, T., and Murata, H. 1987. Morphological studies of experimental arteritis—relation with coronary arteritis in Kawasaki disease—. Angiology **27**: 625–633.
3) Borgmann, S., Endisch, G., Hacker, U.T., Song, B.S., and

Fricke, H. 2003. Proinflammatory genotype of interleukin-1 receptor antagonist is associated with ESRD in proteinase 3-ANCA vasculitis patients. Am. J. Kidney Dis. **41**: 933–942.
4) Gonzalez-Gay, M.A., Di Giovine, F.S., Silvestri, T., Amoli, M.M., Garcia-Porrua, C., Thomson, W., Ollier, W.E., and Hajeer, A.H. 2002. Lack of association between IL-1 cluster and TNF-alpha gene polymorphism and giant cell arteritis. Clin. Exp. Rheumatol. **20**: 431.
5) Gu, L., Weinreb, A., Wang, X.P., Zack, D.J., Qiao, J.H., Weisbart, R., and Lusis, A.J. 1998. Genetic determinants of autoimmune disease and coronary vasculitis in the MRL-lpr/lpr mouse model of systemic lupus erythematosus. J. Immunol. **161**: 6999–7006.
6) Hamashima, Y., Tasaka, K., Hoshino, T., Nagata, N., Furukawa, F., Kao, T., and Tanaka, H. 1982. Mite-associated particles in Kawasaki disease. Lancet **2**: 266.
7) Jibiki, T., Terai, M., Shima, M., Ogawa, A., Hamada, H., Kanazawa, M., Yamamoto, S., Oana, S., and Kohno, Y. 2001. Monocyte chemoattractant protein 1 gene regulatory region polymorphism and serum levels of monocyte chemoattractant protein 1 in Japanese patients with Kawasaki disease. Arthritis Rheum. **44**: 2211–2212.
8) Kamizono, S., Yamada, A., Higuchi, T., Kato, H., and Itoh, K. 1999. Analysis of tumor necrosis factor-alpha production and polymorphisms of the tumor necrosis factor-alpha gene in individuals with a history of Kawasaki disease. Pediatr. Int. **41**: 341–345.
9) Kawasaki, T., Kosaki, F., and Okawa, S. 1974. A new infantile acute febrile mucocutaneous syndrome (MCLS) prevailing in Japan. Pediatrics **54**: 271–276.
10) Lander, E., and Kruglyak, L. 1995. Genetic dissection of complex traits: guidelines for interpreting and reporting linkage results. Nat. Genet. **11**: 241–247.
11) Meissner, H.C., and Leung, D.Y. 2000. Superantigens, conventional antigens and the etiology of Kawasaki syndrome. Pediatr. Infect. Dis. **19**: 91–94.
12) Meyrick, B., Christman, B., and Jesmok, G. 1991. Effects of recombinant tumor necrosis factor-alpha on cultured pulmonary artery and lung microvascular endothelial monolayers. Am. J. Pathol. **138**: 93–108.
13) Murata, H. 1979. Experimental *Candida*-induced arteritis in mice, relation to arteritis in the mucocutaneous lymph node syndrome. Microbiol. Immunol. **23**: 825–831.
14) Naoe, S., Atobe, T., and Murata, H. 1983. Experimental coronary arteritis induced by an alkali extract of *Candida albicans* in stool of Kawasaki disease patient. Pediatr. Jpn. **23**: 257–261.
15) Naoe, S., Takahashi, K., Masuda, H., and Tanaka, N. 1991. Kawasaki disease. With particular emphasis on arterial lesions. Acta Pathol. Jpn. **41**: 785–797.
16) Ohkuni, H., Todome, Y., Mizuse, M., Ohtani, N., Suzuki, H., Igarashi, H., Hashimoto, Y., Ezaki, T., Harada, K., and Imada, Y. 1993. Biologically active extracellular products of oral viridans streptococci and the aetiology of Kawasaki disease. J. Med. Microbiol. **39**: 352–362.
17) Okawara, I.A., Oharaseki, T., Takahashi, K., Hashimoto, Y., Aratani, Y., Koyama, H., Maeda, N., Naoe, S., and Suzuki, K. 2001. Contribution of myeloperoxidase to coronary artery vasculitis associated with MPO-ANCA production. Inflammation **25**: 381–387.
18) Schuger, L., Varani, J., Marks, R.M., Kunkel, S.L., Johnson, K.J., and Ward, P.A. 1989. Cytotoxicity of tumor necrosis factor-alpha for human umbilical vein endothelial cells. Lab. Invest. **61**: 62–68.
19) Takahashi, K., Oharaseki, T., and Naoe, S. 2001. Pathological study of postcoronary arteritis in adolescents and young adults: with reference to the relationship between sequelae of Kawasaki disease and atherosclerosis. Pediatr. Cardiol. **22**: 138–142.
20) Takahashi, K., Oharaseki, T., Wakayama, M., Yokouchi, Y., Naoe, S., and Murata, H. 2004. Histopathological features of murine systemic vasculitis caused by *Candida albicans* extract—an animal model of Kawasaki disease. Inflamm. Res. **53**: 72–77.
21) Yamada, A., Miyazaki, T., Lu, L.-M., Ono, M., Ito, R.M., Terada, M., Mori, S., Hata, K., Nozaki, Y., Nakatsuru, S., Nakamura, Y., Onji, M., and Nose, M. 2003. Genetic basis of tissue specificity of vasculitis in MRL/lpr mice. Arthritis Rheum. **48**: 1445–1451.
22) Yoshioka, T., Matsutani, T., Toyosaki, M.T., Suzuki, H., Uemura, S., Suzuki, R., Koike, M., and Hinuma, Y. 2003. Relation of streptococcal pyogenic exotoxin C as a causative superantigen for Kawasaki disease. Pediatr. Res. **53**: 403–410.

NANO LETTERS

2004
Vol. 4, No. 11
2163−2169

Physicochemical Properties and Cellular Toxicity of Nanocrystal Quantum Dots Depend on Their Surface Modification

Akiyoshi Hoshino,[†,‡,§] Kouki Fujioka,[†] Taisuke Oku,[†] Masakazu Suga,[†] Yu F. Sasaki,[∥] Toshihiro Ohta,[⊥] Masato Yasuhara,[‡] Kazuo Suzuki,[§] and Kenji Yamamoto*[,†,‡]

Department of Medical Ecology and Informatics, Research Institute, International Medical Center of Japan, Toyama 1-21-1, Shinjuku, Tokyo 162-8655, Japan, Department of Pharmacokinetics and Pharmacodynamics, Hospital Pharmacy, Tokyo Medical and Dental University Graduate School, Yushima 1-5-45, Bunkyo-ku, Tokyo 113-8519, Japan, Department of Bioactive Molecules, National Institute of Infectious Diseases, Toyama 1-23-1, Shinjuku, Tokyo 162-8640, Japan, Faculty of Chemical and Biological Engineering, Hachinohe National College of Technology, Tamonoki Uwanotai 16-1, Hachinohe, Aomori 039-1192, Japan, and School of Life Science, Tokyo University of Pharmacy and Life Science, Horinouchi 1432-1, Hachioji, Tokyo 192-0392, Japan

Received August 9, 2004; Revised Manuscript Received October 5, 2004

ABSTRACT

Nanocrystal quantum dots (QDs) have been applied to molecular biology because of their greater and longer fluorescence. Here we report the potential cytotoxicity of our characterized QDs modified with various molecules. Surface modification of QDs changed their physicochemical properties. In addition, the cytotoxicity of QDs was dependent on their surface molecules. These results suggested that the properties of QDs are not related to those of QD-core materials but to molecules covering the surface of QDs.

The behavior of QDs in biological systems is not dependent on the chemical properties of surface-covered molecules but on the nanocrystal particle itself. The surface treatment of nanocrystals (surface-covered functional groups and biomolecules covering the surface of QDs) has specified the biological behavior of whole nanocrystal QDs.

With the development of nanotechnology engineering, nanomaterial products such as carbon nanotubes, fullerenes, and nanocrystal quantum dots (QDs) are now widely produced and consumed. Great quantities of those "artificial nanomaterials" have been used on the premise of being biologically and environmentally harmless, although only a few studies have reported the cellular toxicity of those materials.[1] These artificial nanomaterials are so small that they may be easily spread, stored in the environment and even in our body, and disrupt some functions of living organism consisting of complicated natural nanomaterials. It cannot be denied that these artificial nanomaterials are also detrimental, once small substances such as asbestos, coarse particulates, and particle matter exhaust from diesel engines proved to be harmful.[2−4] Thus, we need to investigate the potential toxicity of artificial nanomaterials.

QDs are now becoming widely used in biotechnology and medical applications.[5−12] QDs have several advantages over organic fluorophores with regard to high luminescence, stability against photobleaching, and a range of fluorescence wavelengths from blue to infrared depending on the particle size.[13] However, QDs aggregate easily and lose luminescence in an intracellular environment, even under acidic (pH < 5) or isotonic conditions. Therefore, it was considered difficult to replace conventional organic fluorescent probes completely with QDs.[14] Recently, some improvements were reported to prevent aggregation under intracellular conditions by the conjugation of biomolecules with QDs,[15−18] and some are used in immunohistochemical staining.[17−19] In this study, we developed several novel surface-modified QDs using carboxylic acids, polyalcohols, and amines and evaluated their physicochemical character and cytotoxicity. There are few

* Corresponding author. E-mail: backen@ri.imcj.go.jp. Tel: +81-3-3202-7181 ext 2856. Fax: +81-3-3202-7364.
† International Medical Center of Japan.
‡ Tokyo Medical and Dental University Graduate School.
§ National Institute of Infectious Diseases.
∥ Hachinohe National College of Technology.
⊥ Tokyo University of Pharmacy and Life Science.

10.1021/nl048715d CCC: $27.50
Published on Web 10/16/2004

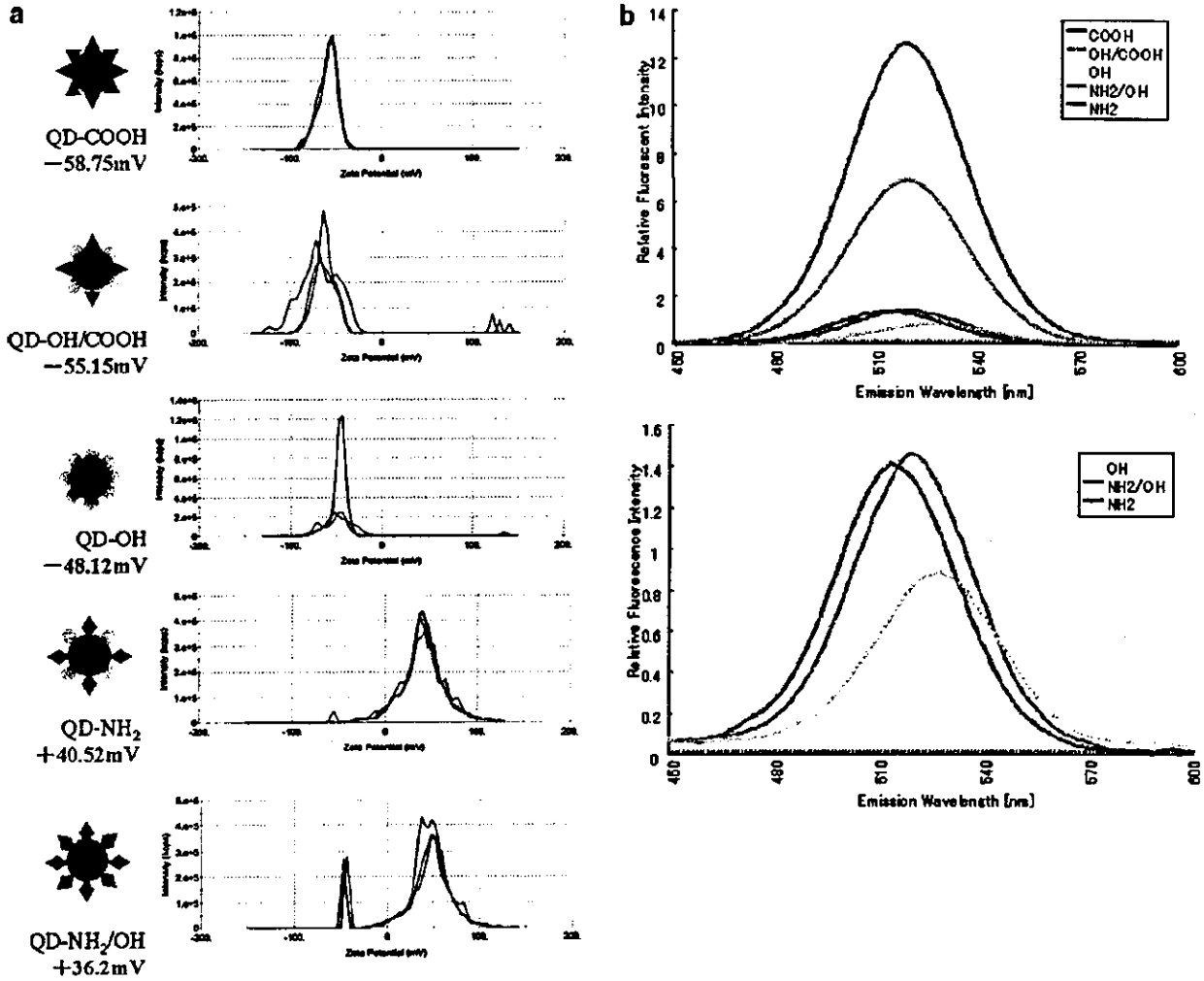

Figure 1. Surface ζ potential and fluorescence intensity of QDs varied by their surface modification. (a) Cartoon (left) and ζ potential (right) of the novel modified QDs. Surface zeta-potential of QDs is measured by electrophoresis. Each line shows the electrophoretic mobility of QDs in the stationaly layers. The data are the average of 30 assays. (b) Relative fluorescence intensity and peak wavelength of QDs measured by fluorescence spectrometry. (Lower) enlarged panel of QD-OH (yellow); QD-NH_2/OH (green) and QD-NH_2 (blue) in the upper panel. The peak emission wavelengths of QD-COOH, QD-OH/COOH, QD-OH, QD-NH_2/OH, and QD-NH_2 varied at 519, 520, 526, 520, and 513 nm, respectively.

studies on the cytotoxicity of QDs in mammalian cells, although several experiments applying to living cells and animals have already been performed.[19−25] In this study, we tested the cytotoxic potential of QDs by three different assays: comet assay, flow cytometry, and MTT assay. The comet assay, which detects DNA damage by gel electrophoresis, has been widely used to detect apoptotic cell damage induced by chemicals.[26−29] In this assay, DNA fragments can be observed as a stream from the nucleus, and the level of damage can be quantitated by the length of the stream of DNA fragments. We report here that the cytotoxicity of QDs is also caused by the surface-covering molecules of QDs but not by the nanocrystalline particle itself.

We synthesized ZnS-coated CdSe nanocrystal QDs (518-nm fluorescence peak emission). Synthesized QDs were then coated with MUA (QD-COOH), cysteamine (QD-NH_2), or thioglycerol (QD-OH) using thiol-exchange reactions as previously described.[30−32] To introduce two functional groups (QD-OH/COOH, and QD-NH_2/OH), we used equal molar quantities of thioglycerol and MUA or cysteamine and thioglycerol, respectively. To investigate the physicochemical properties of these five types of modified QDs, we measured the fluorescence intensity, particle diameter, and surface ζ potential. At first, we assessed the surface ζ potential of QDs to confirm whether the exchange reaction was performed (Figure 1a). As expected, QD-COOH and QD-OH/COOH were highly negatively charged, whereas QD-NH_2 and QD-NH_2/OH were positively charged. QD-OH was less negatively charged than the carboxylic acid groups. QDs with both hydroxyl and carboxyl/amine groups had median charge in both groups. We then assessed whether the difference in the surface modification of QDs affected the fluorescence intensity. The fluorescence intensity and peak wavelength

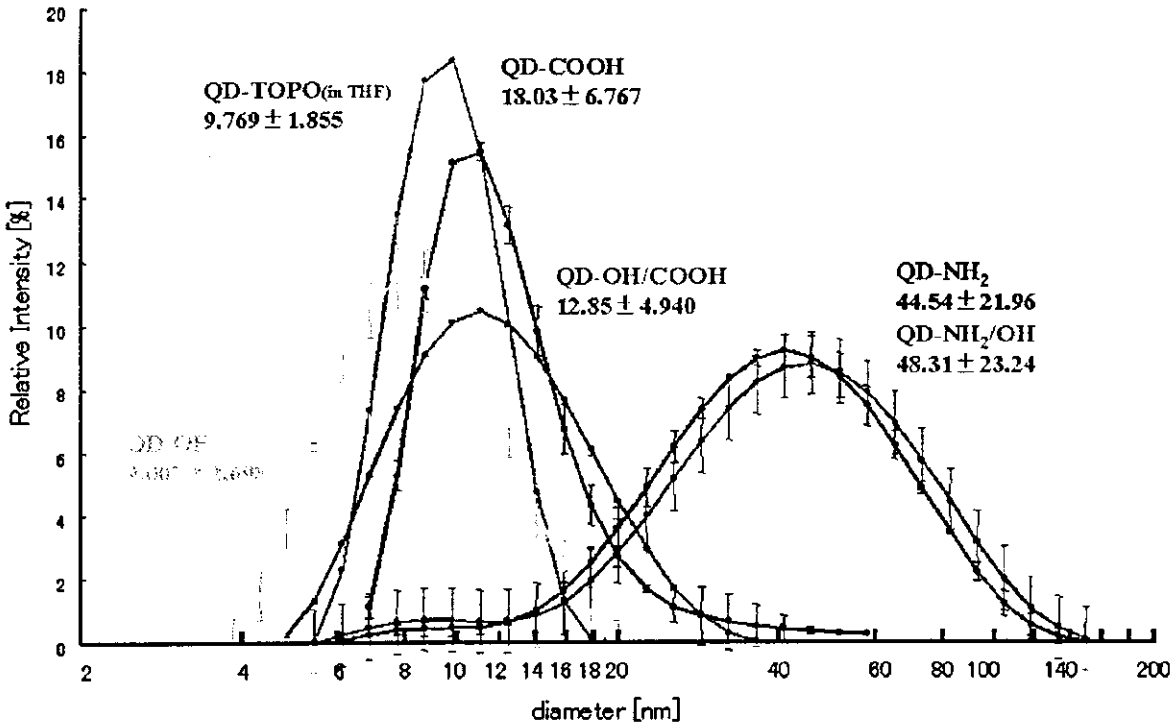

Figure 2. Size distribution of modified QDs in aqueous solution varied by their surface modification. The profile for the distribution of QDs in aqueous solution was observed by dynamic light scattering methods. Values are the mean ± standard deviation of the data measured 12 times, respectively.

were measured using a fluorescence spectrometer (Figure 1b). The QDs of carboxyl groups had higher luminescence than the other groups. Furthermore, the peak wavelength varied according to the surface modification. QDs containing amino groups emitted a shorter wavelength than the originally synthesized QD (TOPO capped-QD; 518-nm emission). In contrast, QDs with hydroxyl groups were slightly red-shifted. We assumed that a longer carbon chain and the carboxyl groups of MUA may contribute to the long lifetime and high quantum yield of QD-COOH. In contrast, the decreasing fluorescence of amino-QD particles may be caused by the oxidation of QD-metal because of the leakage of electrons from QDs through NH_2 groups in aqueous solution.[13] This suggested that the luminescence intensity of QDs may increase according to the surface-covered molecule structures.

Although it is known that the fluorescence of QDs depends on the particle size, the interparticle conformation of QDs in aqueous solution has not yet been revealed. To investigate whether any change in the particle conformation of QDs occurred in the process of surface modification, we attempted to measure the particle diameter of QDs by dynamic light scattering (DLS). We used a He−Ne laser (633-nm wavelength) light source because using a short wavelength that excites the QDs impedes the detection of QD light scattering. The size distribution of QDs was widely spread according to their modifications (Figure 2). Amino-QDs showed a broad particle distribution around 40 nm. In contrast, QDs of carboxyl groups had a narrow distribution around 20 nm. These results seemed to be contradicted by the observation that the emission wavelength of QDs depended on their particle size.[11,34] In addition, it was previously reported that transmission electron microscopy showed the diameter of the uncoated green nanocrystalline QD to be approximately 3.5 nm.[31] Positively charged amino-QDs and negatively charged impure materials in solution (such as TOPO) may form an ionic combination and affect the "apparent" diameter of the particles. In the case of carboxyl QDs, hydrophobic interaction among long carbon chains is also concerned with their larger particle distribution.

Processing the QD surface with hydroxyl group resulted in improved dispersion and stability under hypertonic conditions (Figure 3). In contrast, all of the QDs were stable in nonelectrolyte solutions. All of the modified QDs were stable for 30 min under weak alkaline conditions, whereas only QDs of the amine groups were stable under acidic conditions. These results were useful for advanced surface development to apply QDs in biological and medical fields.

To examine whether QDs affected cell proliferation, we first assessed cell proliferation by MTT assay. The reduction activity of cells was decreased by adding the crude QDs (Figure 4), but we cannot determine whether the amine-QDs were harmful because MTT reagensts were nonbiologically reduced to hormazan by the amine-QDs (data not shown). Then we determined whether this damage was caused by cell death or the suppression of cell activity. To examine whether the cell damage of QDs was affected by their surface potential, the cytotoxicity was evaluated by flow

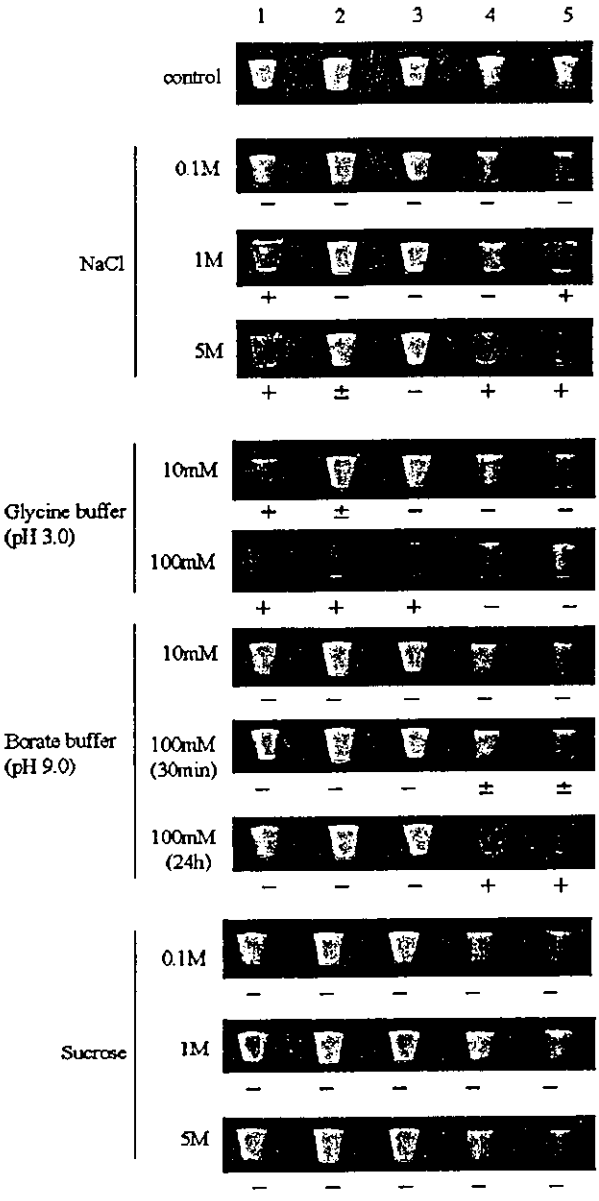

Figure 3. Physicochemical stability of various modified QDs in aqueous buffers. A QD aqueous solution (10 μM) was diluted by the indicated buffers (QD final concentration 100 nM), and incubated for 30 min at room temp. The snapshots were captured using a digital camera with $^1/_{30}$ s exposure excited by a 365-nm wavelength (UV-A). The results were reproduced in three separate experiments. 1, QD-COOH; 2, QD-OH/COOH; 3, QD-OH, 4, QD-NH_2/OH; 5, QD-NH_2; +, aggregated; ±, partially aggregated; −, not aggregated.

cytometry (Figure 5). QDs were introduced into cells by an endocytotic mechanism by adding culture media.[14,25] Cell death was observed by adding crude QDs. In contrast, low cell damage and high labeling efficiency were achieved by adding purified QDs. However, slight cell death was observed only by purified QD-COOH. This cytotoxicity may be caused by uptake QDs located in endosomes.[14] As surface molecules were bound to QDs through the electric interaction

Table 1. DNA-Damaging Effects of the Ingredients and Impurities of the QD Samples

compound	dose (μg/mL)	tail length of 50 nuclei (mm, mean ⊥ SE) 2-h treatment	12-h treatment
MUA	0	23.4 ± 1.05	23.9 ± 1.21
	25	25.6 ⊥ 0.58	28.1 ⊥ 1.31
	50	33.8 ± 2.38[a]	41.2 ± 3.31[a]
	100	54.6 ± 3.27[a]	toxic
	200	76.0 ± 3.52[a]	toxic
	400	80.3 + 3.18[a]	toxic
cysteamine	0	23.5 ⊥ 0.81	24.1 ⊥ 1.05
	50	22.4 ± 0.40	25.1 ± 1.12
	100	23.4 ± 0.95	29.6 ± 1.72
	200	22.9 ± 0.90	35.4 ± 2.89[a]
	400	23.3 ± 0.82	44.5 ± 2.21[a]
thioglycerol	0	23.5 ± 0.81	24.1 ± 1.05
	50	24.7 ± 1.06	27.0 ± 1.65
	100	26.0 ± 1.28	24.7 ± 1.24
	200	22.4 + 0.83	24.6 + 0.99
	400	23.1 ⊥ 0.98	28.1 ⊥ 1.84
TOPO	0	23.8 ± 0.91	23.1 ± 1.04
	50	24.9 ± 0.47	22.5 ± 0.56
	100	27.1 ± 1.33	26.3 ± 1.81
	200	29.6 + 1.92	28.1 + 1.33
	400	32.5 ± 1.43[a]	31.7 ± 1.31[a]
ZnS	0	23.8 ± 0.91	23.1 ± 1.04
	50	23.7 ± 0.89	24.1 ± 0.51
	100	22.5 ± 0.53	22.4 ± 0.34
	200	24.1 ⊥ 0.71	24.1 ⊥ 0.56
	400	23.3 ± 0.54	22.2 ± 0.97

[a] $P < 0.05$.

between the sulfhydryl group and QD-covered zinc,[25] surface molecules such as MUA may be detached by acidic and oxidative conditions in endosomes and released into cytoplasm.[34] The fluorescence of QDs was lost by low pH, by oxidation of the surface structures, or by some intracellular factors adsorbed onto QDs,[13] implying that the advanced development of the surface modification of QDs needs to overcome the cytotoxicity. However, this detachment could be utilized to release valuable materials such as medicines and genes into cells by cellular oxidative/reductive conditions.

Next, to investigate whether cell death by QDs was carried out by an apoptotic pathway, we evaluated the genotoxic potential of QDs by comet assay with WTK1 cells.[27−29] A significant increase in the tail length was observed after 2 h of treatment with QD-COOH at 2 μM (Figure 6a). After treatment for 12 h, the tail length was equal to that of the control cells, suggesting that the induced DNA damage was efficiently repaired during prolonged incubation. Crude QD-COOH samples prepared by only membrane filtration, but not by ultrafiltration, showed stronger DNA damage than purified QD-COOH (Figure 6b). However, QD-NH2, QD-OH, QD-OH/COOH, and QD-NH2/OH induced no DNA damage up to a dose of 4 μM for 2 h. To determine whether the genotoxicity of QDs was caused by QD particles themselves, three ingredients of the QD samples (MUA, cysteamine, and thioglycerol) and two possible impurities (TOPO and ZnS) were also assayed. As shown

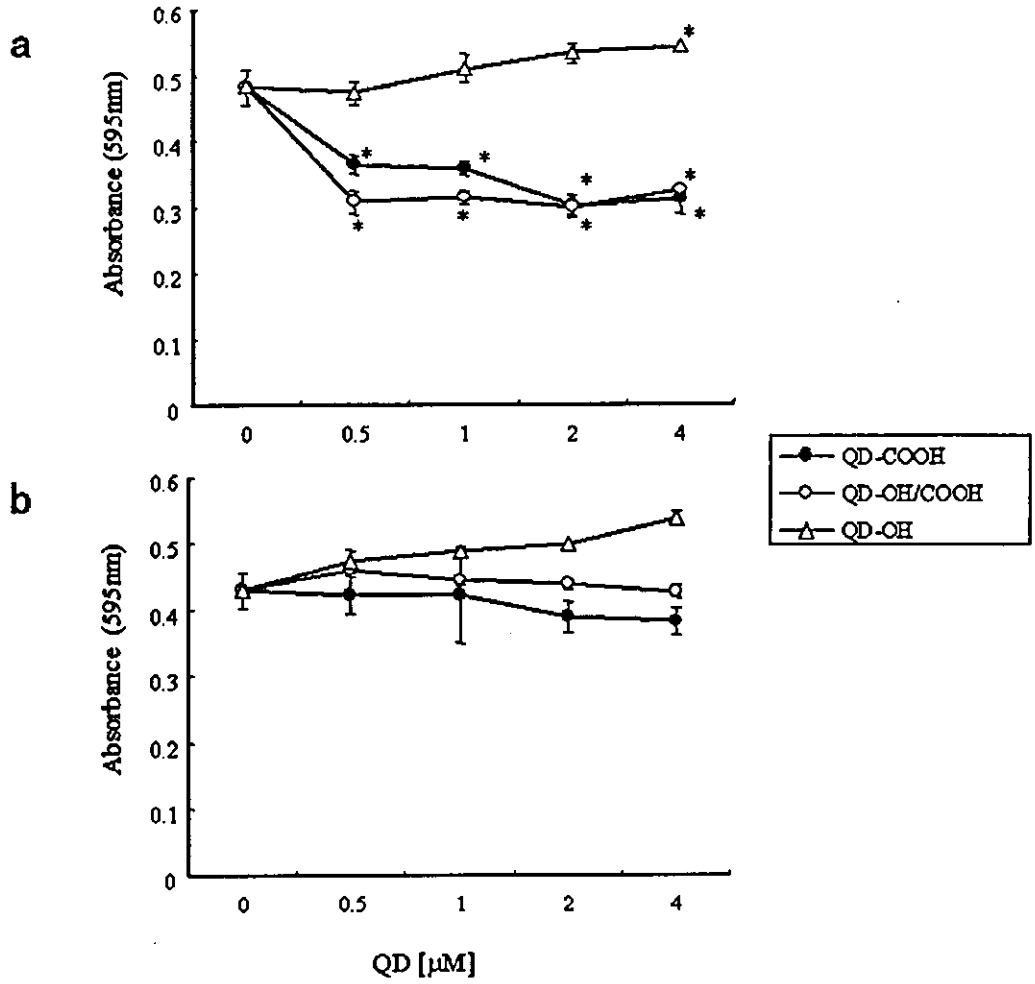

Figure 4. Contaminated impurities and ingredients in QD samples suppress the proliferation of cultured cells. Vero cells were plated at 5×10^4 cells on 96-well plates and cultured for 4 h with (a) crude QD and (b) ultrafiltartion-purified QDs in coexisting MTT reagents (Roche Diagnostics). After incubation, the cells were lysed on the plate, and 595-nm absorbance (reduced hormazan) was measured with a microplate reader. Data are presented as the mean ± standard deviation of duplicate samples. Significance was evaluated by the *t* test versus negative control. *, $p < 0.05$.

in Table 1, treatment with MUA for 12 h caused severe cytotoxicity at doses greater than 100 μg/mL (approximately coordinated to 4μM QD-COOH). DNA damage was observed at doses greater than or equal to 50 μg/mL with 2 h of treatment. Cysteamine was weakly genotoxic when cells were treated for 12 h. Thioglycerol was negative in the assay, suggesting that QD-OH was the least toxic QD among them. Because TOPO was also found to be a cytotoxic and genotoxic compound, the complete removal of TOPO from the QD samples is important in reducing toxicity. These results provided evidence that some hydrophilic compound-coated QDs are responsible for the genotoxicity of QD. Almost all of the DNA damage induced by QD-COOH was efficiently repaired in the cells because DNA damage detected by the comet assay did not persist in the cells treated for 12 h. However, the possibility remains that a few nonrepaired DNA lesions can result in gene mutations or chromosome aberrations. These results provided evidence that some hydrophilic compound-coated QDs are responsible for the cytotoxicity of QDs. It is an important factor for designing less-toxic QDs to select hydrophilic compounds to dissolve QDs in water. These results suggested that the surface treatment of nanocrystals (surface-covered functional groups and biomolecules covered the surface of QDs) has specified the biological behavior of whole nanocrystal QDs.

Nanocrystal QDs have the great potential to be applied to molecular biology and bioimaging because of several advantages over organic fluorophores. As of now, the potential toxicity of industrial products is not considered, whereas the pharmaceutical preparations cannot be commercialized without strictly investigating detrimental effect to human, resulting in the environmental pollution that was caused by the leakage of toxic substance from scrapped industrial products. We the manufacturers must be responsible for characterizing the potential environmental effects and biological toxicity of novel nanomaterial products for industrial laborers and consumers before products are widely

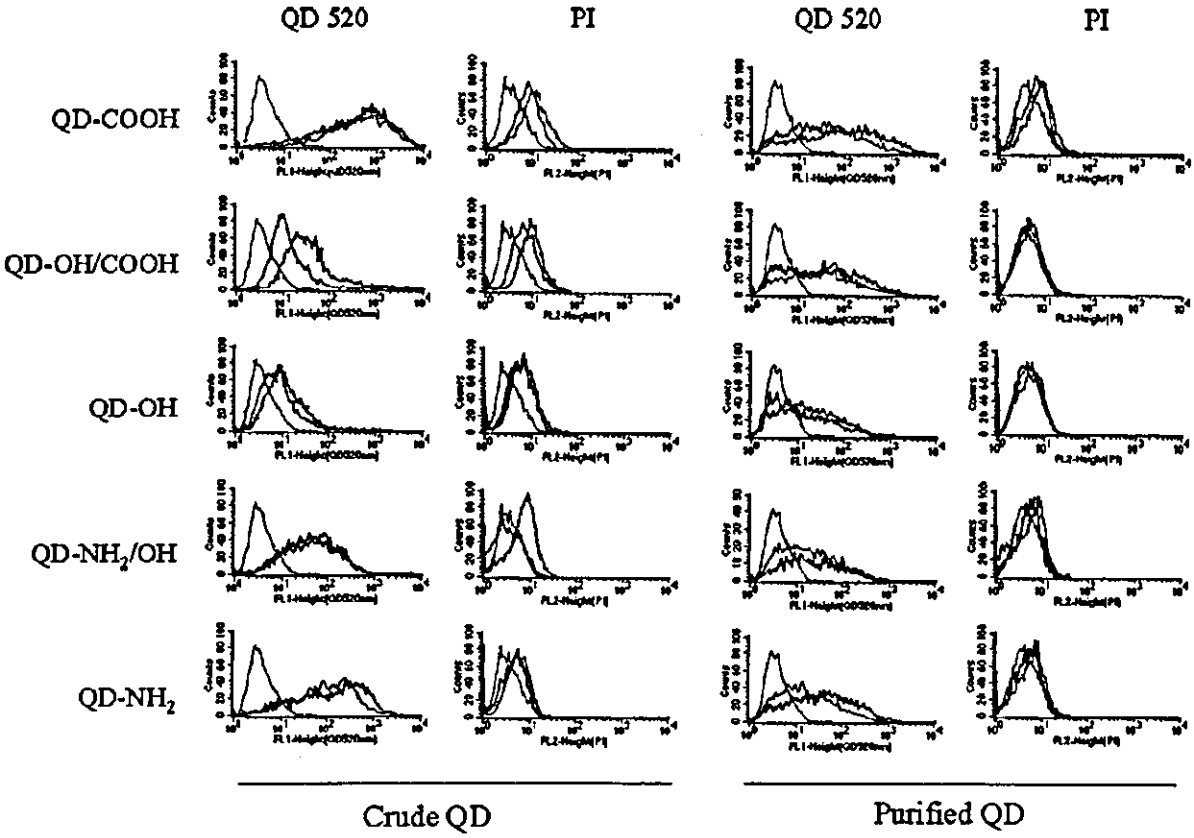

Figure 5. Contaminated impurities and ingredients in QD samples induce cell death. Vero cells were plated at 1×10^5 cells on 24-well plate and incubated for 12 h with crude QDs and ultrafiltration-purified QDs at 2 μM (red line) and 1 μM (blue line). Then cells were harvested, stained with propidium iodide, and analyzed by flow cytometry. The x axis indicates the fluorescence intensity of QDs (left columns) and PI (right columns) on a log scale. The green line shows untreated cells as a negative control. Results are representative of three separate experiments.

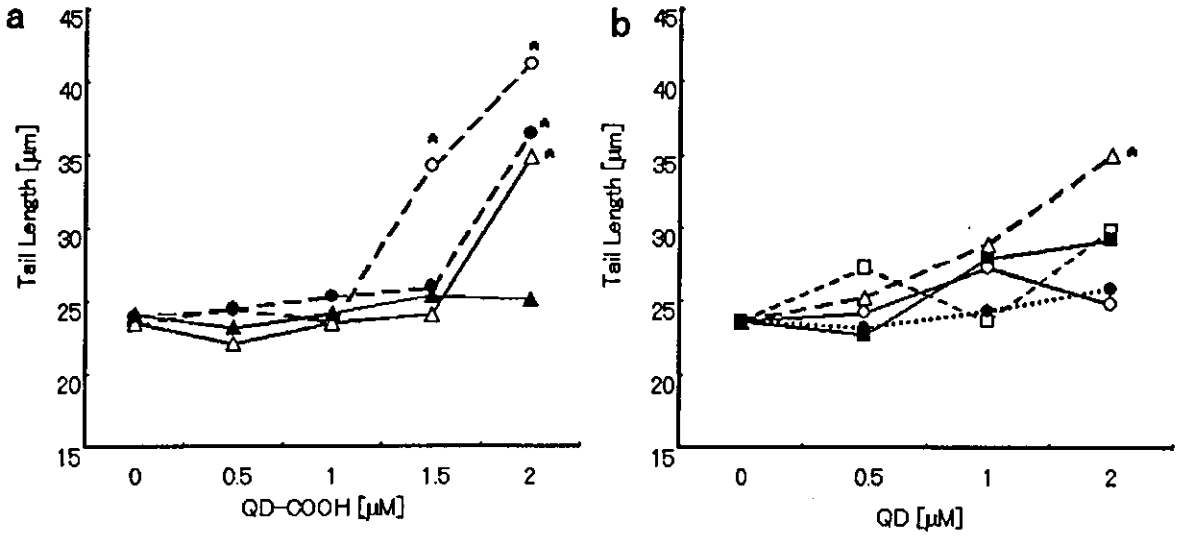

Figure 6. DNA-damaging effects of hydrophilic nanocrystalline QDs by comet assay. (a) WTK-1 cells were treated with QD-COOH (ultrafiltration purified; ▲, △) or QD-COOH (crude; ●, ○) for 2 h (open symbols) and 12 h (filled symbols). Then cells were harvested and embedded in 1% agarose, and electrophoresis was performed at 0 °C for 20 min at 25 V (0.96 V/cm) and approximately 250 mA. After being stained with ethidium bromide, the length of the whole comet was measured for 50 nuclei for each dose using a fluorescence microscope (200× magnification). (b) Cells were treated with QD-COOH (△), QD-NH_2 (□), QD-OH (○), QD-OH/COOH (●), or QD-NH_2/OH (■) for 2 h. The difference between the means in the treated and control plates was compared with the Dunnett test after one-way ANOVA. *, $p < 0.05$.

commercialized. In this paper, we revealed that the toxicity of QDs in biological systems is not dependent on the nanocrystal particle itself but on the surface molecules. In the case of QDs, no cytotoxicity was detected from their ingredients or the QD core itself, suggesting that surface processing will overcome the toxicity of nanomaterials. Less cytotoxicity derived from their ingredients or the QD core itself was observed in QD-OH in vitro. It is expected that QDs will be applied in the biomedical field for the innovative investigation, diagnosis, and medical treatment of various diseases.[9-12] When producing nanometer-sized materials in the future, it will be vital that the behavior of QDs in the biological system is not dependent on the chemical properties of surface-covered molecules but on the nanocrystalline particle itself. Surface modifications of functional molecules combined with nanoparticles may work as bionanomachines conforming to the functions designated by their surface molecules.

We conclude that the surface treatment of nanocrystals (surface-covered functional groups and biomolecules covering the surface of QDs) has specified the biological behavior of whole nanocrystalline QDs. We hope that the surface modifications of functional molecules combined with nanoparticles may work as a bionanomachine conforming to the functions designated by their surface molecules.

Acknowledgment. We are grateful to Dr. Akira Yuo and Dr. Taeko Dohi (Research Institute, IMCJ) for generously providing valuable advice about data collection. We thank Dr. Yukio Yamaguchi and colleagues (Department of Chemical System Engineering, University of Tokyo) for amino-QD improvements. This work was supported by a Medical Techniques Promotion Research Grant from the Ministry of Health, Labor and Welfare of Japan (H14-nano-004).

Supporting Information Available: Experimental procedures: Preparation of CdSe/ZnS fluorescent nanocrystal Qdots, preparation of surface-modified nanocrystal QDs, and protocols for comet assay and cell viability assays. This material is available free of charge via the Internet at http://pubs.acs.org.

References

(1) Colvin, V. L. *Nat. Biotechnol.* **2003**, *21*, 1166−1170.
(2) Borm, P. J. *Inhalation Toxicol.* **2002**, *14*, 311−324.
(3) Albrecht, C.; Borm, P. J.; Adolf, B.; Timblin, C. R.; Mossman, B. T. *Toxicol. Appl. Pharmacol.* **2002**, *184*, 37−45.
(4) Schins, R. P.; Duffin, R.; Hohr, D.; Knaapen, A. M.; Shi, T.; Weishaupt, C.; Stone, V.; Donaldson, K.; Borm, P. J. *Chem. Res. Toxicol.* **2002**, *15*, 1166−1173.
(5) Rosenthal, S. J.; Tomlinson, I.; Adkins, E. M.; Schroeter, S.; Adams, S.; Swafford, L.; McBride, J.; Wang, Y.; DeFelice, L. J.; Blakely, R. D. *J. Am. Chem. Soc.* **2002**, *124*, 4586−4594.
(6) Dubertret, B.; Skourides, P.; Norris, D. J.; Noireaux, V.; Brivanlou, A. H.; Libchaber, A. *Science* **2002**, *298*, 1759−1762.
(7) Jaiswal, J. K.; Mattoussi, H.; Mauro, J. M.; Simon, S. M. *Nat. Biotechnol.* **2003**, *21*, 47−51.
(8) Xu, H.; Sha, M. Y.; Wong, E. Y.; Uphoff, J.; Xu, Y.; Treadway, J. A.; Truong, A.; O'Brien, E.; Asquith, S.; Stubbins, M.; Spurr, N. K.; Lai, E. H.; Mahoney, W. *Nucleic Acids Res.* **2003**, *31*, 43.
(9) Wu, X.; Liu, H.; Liu, J.; Haley, K. N.; Treadway, J. A.; Larson, J. P.; Ge, N.; Peale, F.; Bruchez, M. P. *Nat. Biotechnol.* **2003**, *21*, 41−46.
(10) Chan, W. C.; Maxwell, D. J.; Gao, X.; Bailey, R. E.; Han, M.; Nie, S. *Curr. Opin. Biotechnol.* **2002**, *13*, 40−46.
(11) Zhu, L.; Ang, S.; Liu, W. T. *Appl. Environ. Microbiol.* **2004**, *70*, 597−598.
(12) Mattoussi, H.; Mauro, J. M.; Goldman, E. R.; Anderson, G. P.; Sundar, V. C.; Mikulec F. V.; Bawendi, M. G. *J. Am. Chem. Soc.* **2000**, *122*, 12142−12150.
(13) Gerion, D.; Pinaud, F.; Williams, S. C.; Parak, W. J.; Zanchet, D.; Weiss, S.; Alivisatos, A. P. *J. Phys. Chem. B* **2001**, *105*, 8861−8871.
(14) Hanaki, K.; Momo, A.; Oku, T.; Komoto, T.; Maenosono, S.; Yamaguchi, Y.; Yamamoto, K. *Biochem. Biophys. Res. Commun.* **2003**, *302*, 496−501.
(15) Medintz, I. L.; Clapp, A. R.; Mattoussi, H.; Goldman, E. R.; Fisher, B.; Mauro, J. M. *Nat. Mater.* **2003**, *9*, 630−638.
(16) Chan, W. C.; Nie, S. *Science* **1998**, *281*, 2016−2018.
(17) Goldman, E. R.; Balighian, E. D.; Mattoussi, H.; Kuno, M. K.; Mauro, J. M.; Tran, P. T.; Anderson, G. P. *J. Am. Chem. Soc.* **2002**, *124*, 6378−6382.
(18) Gao, X.; Chan, W. C.; Nie, S. *J. Biomed. Opt.* **2002**, *7*, 532−537.
(19) Akerman, M. E.; Chan, W. C.; Laakkonen, P.; Bhatia, S. N.; Ruoslahti, E. *Proc. Natl. Acad. Sci. U.S.A.* **2002**, *99*, 12617−12621.
(20) Larson, D. R.; Zipfel, W. R.; Williams, R. M.; Clark, S. W.; Bruchez, M. P.; Wise, F. W.; Webb, W. W. *Science* **2003**, *300*, 1434−1436.
(21) Mansson, A.; Sundberg, M.; Balaz, M.; Bunk, R.; Nicholls, I. A.; Omling, P.; Tagerud, S.; Montelius, L. *Biochem. Biophys. Res. Commun.* **2004**, *314*, 529−534.
(22) Pellegrino, T.; Parak, W. J.; Boudreau, R.; LeGros, M. A.; Gerion, D.; Alivisatos, A. P.; Larabell, C. A. *Differentiation* **2003**, *71*, 542−548.
(23) Levene, M. J.; Dombeck, D. A.; Kasischke, K. A.; Molloy, R. P.; Webb, W. W. *J. Neurophysiol.* **2004**, *91*, 1908−12.
(24) Dahan, M.; Levi, S.; Luccardini, C.; Rostaing, P.; Riveau, B.; Triller, A. *Science* **2003**, *302*, 442−445.
(25) Hoshino, A.; Hanaki, K.; Suzuki, K.; Yamamoto, K. *Biochem. Biophys. Res. Commun.* **2004**, *314*, 46−53.
(26) Singh, N. P.; McCoy, M. T.; Tice, R. R.; Schneider, E. L. *Exp. Cell. Res.* **1988**, *175*, 184−191.
(27) Sasaki, Y. F.; Tsuda, S.; Izumiyama, F.; Nishidate, E. *Mutat. Res.* **1997**, *388*, 33−44.
(28) Sasaki, Y. F.; Sekihashi, K.; Izumiyama, F.; Nishidate, E.; Saga, A.; Ishida, K.; Tsuda, S. *Crit. Rev. Toxicol.* **2000**, *30*, 629−799.
(29) Tice, R. R.; Agurell, E.; Anderson, D.; Burlinson, B.; Hartmann, A.; Kobayashi, H.; Miyamae, Y.; Rojas, E.; Ryu, J. C.; Sasaki, Y. F. *Environ. Mol. Mutagen.* **2000**, *35*, 206−221.
(30) Hines, M. A.; Guyot-Sionnest, P. *J. Phys. Chem.* **1996**, *100*, 468−471.
(31) Dabboussi, B. O.; Rodriguez-Viejo, J.; Mikulec, F. V.; Heine, J. R.; Mattoussi, H.; Ober, R.; Jensen, K. F.; Bawendi, M. G. *J. Phys. Chem. B* **1997**, *101*, 9463−9475.
(32) Reynolds, C. P.; Biedler, J. L.; Spengler, B. A.; Reynolds, D. A.; Ross, R. A.; Frenkel, E. P. *J. Natl Cancer Inst.* **1986**, *76*, 375−87.
(33) Liber, H. L.; Yandell, D. W.; Little, J. B. *Mutat. Res.* **1989**, *216*, 9−17.
(34) Bruchez, M., Jr.; Moronne, M.; Gin, P.; Weiss, S.; Alivisatos, A. P. *Science* **1998**, *281*, 2013−2016.

NL048715D

IMMUNOPHARMACOLOGY AND IMMUNOTOXICOLOGY
Vol. 26, No. 4, pp. 527–543, 2004

Induction of Coronary Arteritis with Administration of CAWS (*Candida albicans* Water-Soluble Fraction) Depending on Mouse Strains

Noriko Nagi-Miura,[1] Yuko Shingo,[1] Yoshiyuki Adachi,[1] Akiko Ishida-Okawara,[2] Toshiaki Oharaseki,[3] Kei Takahashi,[3] Shiro Naoe,[3] Kazuo Suzuki,[2] and Naohito Ohno, Ph.D.[1,*]

[1]Laboratory for Immunopharmacology of Microbial Products, School of Pharmacy, Tokyo University of Pharmacy and Life Science, Hachioji, Tokyo, Japan
[2]Department of Bioactive Molecules, National Institute of Infectious Diseases, Tokyo, Japan
[3]Department of Pathology, Ohashi Hospital, Toho University School of Medicine, Tokyo, Japan

ABSTRACT

The intraperitoneal administration of CAWS (water-soluble extracellular polysaccharide fraction obtained from the culture supernatant of *Candida albicans*) to mice induces coronaritis similar to Kawasaki disease. We analyzed differences in the production of cytokines involved in the occurrence of coronary arteritis among mouse strains, C3H/HeN, C57BL/6, DBA/2 and CBA/J that were injected with CAWS at 4 mg/mouse for 5 consecutive days in the first week and the fifth week of administration. The incidence of arteritis was 100% in C57BL/6, C3H/HeN and DBA/2 mice, but only 10% in CBA/J mice. The coronary arteritis observed in DBA/2 mice

*Correspondence: Prof. Naohito Ohno, Ph.D., Laboratory for Immunopharmacology of Microbial Products, School of Pharmacy, Tokyo University of Pharmacy and Life Science, 1432-1, Horinouchi, Hachioji, Tokyo 192-0392, Japan; Fax: 81-426-76-5570; E-mail: ohnonao@ps.toyaku.ac.jp.

DOI: 10.1081/IPH-200042295
0892-3973 (Print); 1532-2513 (Online)

was the most serious, with several mice expiring during the observation period. The CAWS-sensitive strains revealed increased levels of IL-6 and IFN-γ during the course of a specific response to CAWS by spleen cells. In contrast, IL-10 levels were observed to increase markedly in CAWS-resistant CBA/J mice, but not the CAWS-sensitive strains. However, TNF-α levels were more elevated only in DBA/2 mice. The difference in disease development and cytokine production strongly suggests that the genetic background of the immune response to CAWS contributes to the occurrence of coronary arteritis.

Key Words: *Candida albicans*; Induction of arteritis; Polysaccharide; DBA/2 mice.

INTRODUCTION

Kawasaki disease, also referred to as acute febrile mucocutaneous lymph node syndrome or MCLS, was first reported by Kawasaki in 1967.[1,2] A disease of unknown cause, it affects mainly children aged 4 and under. The number of patients diagnosed with Kawasaki disease annually is roughly 10,000. The patients present with systemic coronary arteritis, and the greatest concern with this symptom is the occurrence of coronary arteritis or coronaritis, which occurs as a sequela in nearly 10% of all patients.[3,4] Moreover, in the case of the formation of giant coronary aneurysms, complications involving myocardial ischemia and myocardial disorders caused by vascular occlusion due to thrombus formation may arise. In actuality, sudden death due to myocardial infarction occurs in several percent of Kawasaki disease patients. Although the occurrence of such coronary artery disorders has decreased with the introduction of γ-globulin therapy, the mechanism of their occurrence along with the pharmacological mechanism of the treatment is unknown.[5,6]

Murata et al.[7,8] reported that Kawasaki-disease-like coronary arteritis was induced specifically at the origin of the coronary arteries in mice administered an alkaline extract of *C. albicans* isolated from patients (CADS) with Kawasaki disease. Ishida-Okawara et al.[9] have demonstrated that mice with coronary arthritis induced with a CADS injection show an increase in anti-myeloperoxidase (MPO)-specific anti-neutrophil cytoplasmic antibody (MPO-ANCA) in their serum. In addition, MPO was identified to be the antigen to MPO-ANCA using MPO-deficient mice.[9] These findings show the substances including β-glucan derived from *C. albicans* might relate to coronary arteritis.

The number of opportunistic infections is on the rise accompanying the proliferation of highly advanced medical treatment. *Candida* infections are frequently observed in patients in high-risk groups.[10,11] As the chemotherapeutic agent for mycoses is completely different from that for bacterial infections, early diagnosis is critical.[12,13] Since fungal cell wall contains β-glucan as its main component, β-glucan is detected in the blood of patients with deep mycoses. Thus, measurement of β-glucan in the blood is widely used for the early diagnosis of deep mycoses.[14,15] In this study, we cultured *Candida* spp. in completely synthetic media, obtained the water-soluble polysaccharide fraction released into the culture supernatant (*Candida albicans* water-soluble fraction or CAWS), and performed various analyses on that fraction. As a result, CAWS was found to be composed of mannoprotein and a β-glucan complex and to activate the limulus G factor, to exhibit acute lethal toxicity in the case of

intravenous administration, and to activate vascular endothelial cells, platelets and lymphocytes.[16-18] In addition to CADS, other substances in the soluble fraction may cause the development of coronary arteritis in mice.

In the present study, the incidence of coronaritis was found to be higher when CAWS was administered than when the conventional alkaline extract was administered, and a difference in the incidence was observed among mouse strains. We also analyzed the correlation of cytokine production in the development of coronary arteritis induced by CAWS.

MATERIALS AND METHODS

Mice

Male C3H/HeN and DBA/2 mice were purchased from Japan SLC, whereas male C57BL/6 and CBA/J mice were purchased from Charles River Japan. The mice were housed in a specific pathogen-free (SPF) environment and were used in the study at 5-14 weeks of age.

Organisms

Candida albicans strain IFO1385 was purchased from the Institute for Fermentation, Osaka (IFO), stored at 25°C on Sabauroud's agar (Difco, USA) and passaged once every three months.

Preparation of CAWS

CAWS was prepared from *C. albicans* strain IFO1385 in accordance with conventional methods.[18] The procedure used is as follows: 5 L of medium (C-limiting medium) was added to a glass incubator and cultured for 2 days at 27°C while supplying air at a rate of 5 L/min and rotating at 400 rpm. Following the culture, an equal volume of ethanol was added and after the mixture was allowed to stand overnight, the precipitate was collected. The precipitate was dissolved in 250 mL of distilled water, ethanol was added and the mixture was allowed to stand overnight. The precipitate was collected and dried with acetone to obtain CAWS.

Administration Schedule for Induction of Coronary Arteritis

CAWS (0 or 4 mg/mouse) was administered intraperitoneally for 5 consecutive days to each mouse in week 1. In week 5, CAWS (0 or 4 mg/mouse) was again administered in the same manner as that in week 1, after which the mice were sacrificed in week 9. The hearts of the animals were fixed with 10% neutral formalin and prepared in paraffin blocks. Tissue sections were stained with Hemotoxylin-Eosin (HE) stain. Cells were prepared from the spleen and cultured. Cells were also prepared from peritoneal exudative cells (PECs) and from the thymus, and enumerated. Liver weight was measured.

Preparation of Mouse Serum

The mice were anesthetized with chloroform and then sacrificed after which blood was drawn from the heart. After the blood samples had been left to stand for 60 minutes at room temperature and then for 60 minutes at 4°C, they were separated by centrifugation at 15,000 rpm × 10 minute, and the resulting supernatant was used as the serum. All the samples were stored at −25°C or lower.

CAWS-Specific Reaction in the Isolated Spleen Cells

The mice were anesthetized and then sacrificed, after which the spleen was excised. After teasing using a mesh in RPMI-1640 medium, the tissue was separated by centrifugation at 1200 rpm × 5 minute, and the resulting cells were treated with ACK-lysing buffer (NH_4Cl 8.20 g/L, $KHCO_3$ 1 g/L, EDTA·2Na 37.2 mg/L). After two washes with RPMI medium, the spleen cells were counted to adjust the cell density and then used after being suspended in RPMI medium with 10% FCS (fetal calf serum). The spleen cells were adjusted to 1×10^7 in RPMI 1640 medium containing 10% FCS and 500 µl aliquots were added to each well of a 48-well plate. Following the addition of CAWS (0, 2.5, 5 or 10 µg/ml), the cells were culture for 48 hours in a 5% CO_2 incubator at 37°C. The cytokine level of the culture supernatant was determined by Enzyme-Linked Immuno Sorbent Assay (ELISA) as described below.

Measurement of IL-1β, IL-4, IL-10 and IL-12

The IL-1β level was measured using a Mouse IL-1β ELISA Kit (Biosource International). Levels of IL-4, IL-10 and IL-12 were measured using Mouse IL-4, IL-10 and IL-12 $O_{PT}EIA^{TM}$ Kits (Pharmingen).

Measurement of IL-6

An ELISA 96-well plate (Sumitomo Bakelite) was coated with rat anti-mouse IL-6 mAb (Pharmingen) using 0.1 M bicarbonate buffer (pH 9.5) and incubated overnight at 4°C. After a wash with Phosphate buffered saline with 0.05% Tween 20 (PBST), the antibody was blocked for 40 minutes at 37°C with BPBST. This was followed by the addition of standard and sample (50 µL), incubation for 40 minutes at 37°C and washing with PBST. Fifty microliters of a secondary antibody in the form of biotinylated rat anti-mouse IL-6 mAb (1/2000; Pharmingen) was then added, and after incubation for 40 minutes at 37°C and a wash with PBST, peroxidase-conjugated streptavidin (1/10000; Zymed Laboratories, Inc.) was added. This was followed by incubation for 40 minutes at 37°C and washing with PBST. Subsequently, 50 µL of peroxidase substrate (TMB microwell peroxidase substrate system, KPL Inc.) was added to generate color, and absorbance was measured as previously described. Recombinant mouse IL-6 (Pharmingen) was used as the standard.

Measurement of IFN-γ

An ELISA 96-well plate (Sumitomo Bakelite) was coated with rat anti-mouse IFN-γ monoclonal antibody (mAb; Pharmingen) using 0.1 M $NaHCO_3$ (pH 8.2) and

incubated overnight at 4°C. After a wash with 0.05% Tween-PBS (PBST), the antibody was blocked for 40 minutes at 37°C with 0.5% BSA (bovine serum albumin)-PBST (BPBST). This was followed by the addition of standard and sample (50 μL), incubation for 40 minutes at 37°C and washing with PBST. Fifty microliters of a secondary antibody in the form of biotinylated rat anti-mouse IFN-γ (1/1000; Pharmingen) was then added, and after incubation for 40 minutes at 37°C and a wash with PBST, peroxidase-conjugated streptavidin (1/2000; Pharmingen) was added. This was followed by incubation for 40 minutes at 37°C and washing with PBST. Subsequently, color was generated using peroxidase substrate (TMB microwell peroxidase substrate system, KPL Inc.). After termination of the reaction with 1 M phosphoric acid, absorbance (OD 450/Ref. 630) was measured. Recombinant mouse IFN-γ (Pharmingen) was used as the standard.

Measurement of TNF-α

An ELISA 96-well plate (Nunc) was coated with rat anti-mouse TNF-α mAb (1/500; Pharmingen) using 0.1 M NaH_2PO_4– 0.1 M Na_2HPO_4 buffer (pH 6.0) and incubated overnight at 4°C. After a wash with PBST, the antibody was blocked for 60 minutes at room temperature with BPBST. This was followed by the addition of standard and sample (50 μL), incubation for 3 hours at room temperature and washing with PBST. Fifty microliters of a secondary antibody in the form of biotinylated rat anti-mouse TNF-α mAb (1/1000; Pharmingen) was then added, and after incubation for 60 minutes at room temperature and a wash with PBST, horseradish-peroxidase-conjugated streptavidin (1/1000; Pharmingen) was added. This was followed by incubation for 30 minutes at room temperature and washing with PBST. Subsequently, color was generated and absorbance was measured as previously described. Recombinant mouse TNF-α (Pharmingen) was used as the standard.

Measurement of Anti-CAWS Antibody Titer

An ELISA 96-well plate (Nunc) was coated with CAWS using 0.1 M bicarbonate buffer (pH 9.5) and incubated overnight at 4°C. After a wash with PBST, the antibody was blocked for 60 minutes at 37°C with BPBST and again washed with BPST. A serum sample diluted with BPBST (50 μl) was added, and incubation continued for another 60 minutes at 37°C. After a wash with PBST, 50 μL of peroxidase-conjugated goat anti-mouse IgG + IgM Ab (1/5000; Wako) was added and reaction was allowed to proceed for 60 minutes at 37°C. Color was generated and absorbance was measured as previously described. Furthermore, color generation was stopped after 10 minutes.

Measurement of Antibody Subclass

An ELISA 96-well plate (Nunc) was coated with CAWS using 0.1 M bicarbonate buffer (pH 9.5) and incubated overnight at 4°C. After a wash with PBST, the antibody was blocked for 60 minutes at 37°C with BPBST and again washed with PBST. A serum sample (50 μL) diluted with BPBST was added and incubation continued

for another 60 minutes at 37°C. After a wash with PBST, 50 μL of biotin-conjugated anti-mouse IgG1 (1/1000)-IgG2a (1/3000)-IgM (1/5000) Ab or peroxidase-conjugated anti-mouse IgE Ab (1/500) was added and the reaction was allowed to proceed for 60 minutes at 37°C. With respect to the biotin-conjugated antibody, after a wash with PBST, horseradish-peroxidase-conjugated streptavidin (1/5000; Pharmingen) was added, and incubation was continued for 60 minutes at 37°C. Color was generated and absorbance measured as previously described. Furthermore, color generation was stopped after 10 minutes.

Test for Significant Difference

Tests for significant differences in this study were performed using Student's t-test and values of $P<0.05$ were judged significant.

RESULTS

Development of Coronary Arteritis Induced with CAWS and Difference Among Strains

Administration of CAWS induced the development of coronary arteritis (Fig. 1). The arteritis-inducing activity of CAWS was compared among four mouse strains in accordance with the method of Murata et. al.[7,8] CAWS was dissolved in physiological saline to a concentration of 4 mg/0.2 mL, administered intraperitoneally to each mouse for five consecutive days, and again administered for five consecutive days in week 5, after which the mice were sacrificed in week 9. The tissue sections in the ninth week were prepared from the origin of the coronary arteries of the coronary aorta and stained with HE. The coronary arteritis induced by CAWS was accompanied by hypertrophy of the tunica intima, the rupture of elastic fibers and a diffuse invasion by lymphocytes, histiocytes, fibroblasts, smooth muscle cells and eosinophils of vascular endothelial cells and the regions surrounding blood vessels (Fig. 1). On the basis of such characteristics, the coronary arteritis induced by CAWS was presumed to be the so-called proliferative granulomatous coronary arteritis, and is clearly different from fibrinoid arteritis. Differences in the incidence of coronary arteritis were observed among the mouse strains. The coronary arteritis was observed in all mice of the DBA/2, C57BL/6 and C3H/HeN strains. It was observed to cover nearly the entire periphery of the vessels in DBA/2 mice, and those mice were considered to demonstrate the most virulent form of coronary arteritis (data not shown). On the other hand, CBA/J mice exhibited the lowest incidence of coronary arteritis among the four strains tested (10%), with few sites where coronary arteritis occurred.

Comparison of Survival Rates Among CAWS-Administered Mice

Among the mice administered CAWS according to the coronary arteritis induction protocol, only DBA/2 mice exhibited high mortality. Therefore, the disease

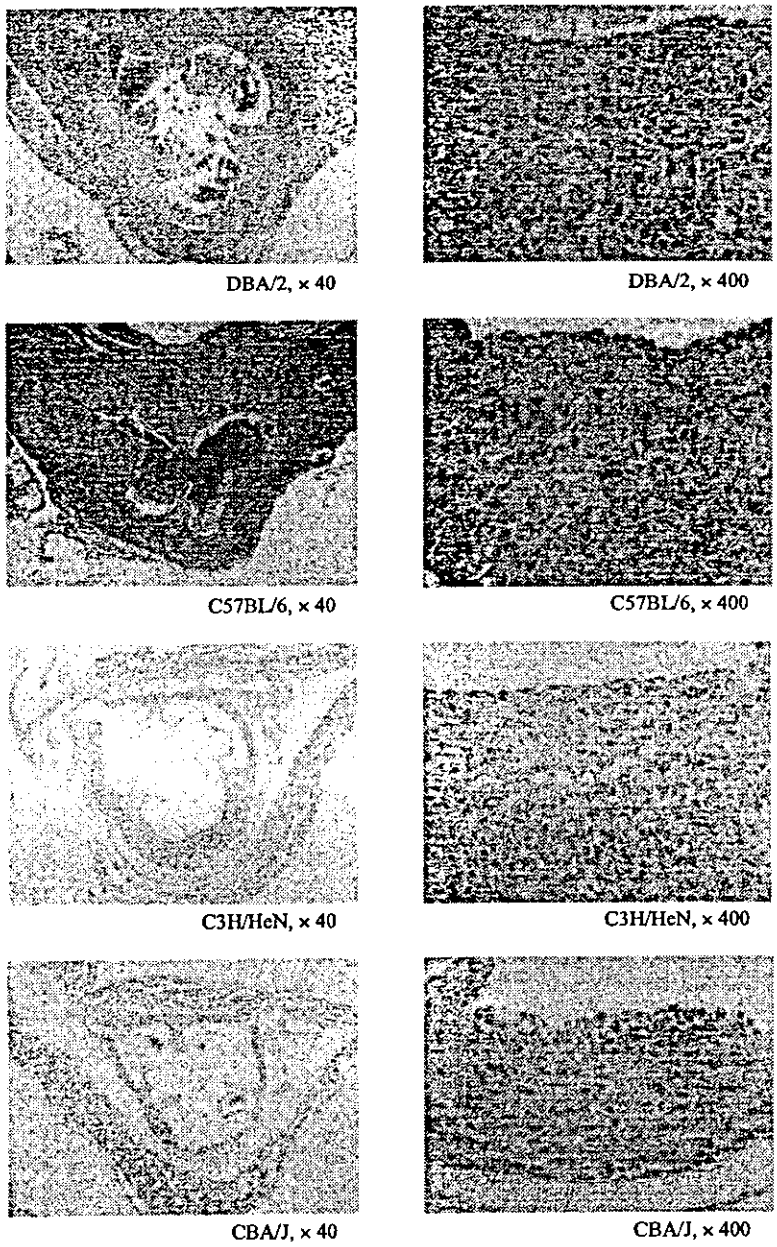

Figure 1. Histological observations of coronary arteritis. CAWS (4 mg/mouse) was administered i.p. to DBA/2, C57BL/6, C3H/HeN and CBA/J mice for five consecutive days in the 1st and 5th week. In the 9th week, mice were sacrificed and prepared sections stained with the hematoxylin-eosin method.

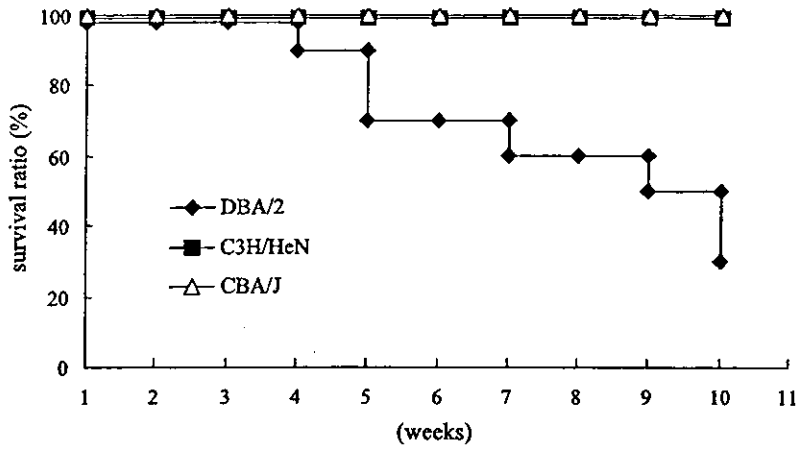

Figure 2. Survival ratio of CAWS-administered mice. CAWS (4 mg/mouse) was administered i.p. to DBA/2, C3H/HeN and CBA/J mice for five consecutive days in the 1st and 5th week. Survival had been observed for ten weeks. (N = 10).

course was examined in DBA/2 mice. DBA/2 mice were confirmed to expire beginning in the fourth week after the start of administration. The number that expired gradually increased and by the ninth week when the mice were assessed for coronary arteritis, the survival rate had dropped to 50%, and ultimately decreased to 30% (Fig. 2).

Tissue sections were prepared from the hearts of expired DBA/2 mice and observed microscopically using the HE stain. In the DBA/2 mice that expired due to administration of CAWS (n = 3), prominent neutrophil and histiocyte invasion was observed, along with the disappearance of striated muscle (Fig. 3A), and in some of the tissue, fibrosis appeared to occur in addition to cellular invasion (Fig. 3B and C); namely, the cause of death was suggested to be myocardial infarction. On the basis of these findings, it was suggested that the most virulent form of coronary arteritis was induced in DBA/2 mice, which resulted in the occurrence of cardiac ischemia that ultimately led to myocardial infarction.

Change of Cell Number in Organs on CAWS-Administration

As we observed a high incidence of cornory arteritis induced with CAWS in three strains, the increase in the numbers of immune cells was determined, along with the weight of the liver. These measurements were made in mice administered CAWS in accordance with the coronary arteritis induction protocol. In the spleen, although splenomegaly was observed in C3H/HeN, DBA/2 and C57BL/6 mice, significant increases in cell counts were exhibited by only C3H/HeN and DBA/2 mice (Fig. 4A). There were no changes in the thymus cell count in any mouse strains (Fig. 4B). In the case of PECs, although the changes were not significant, all strains exhibited an increase (Fig. 4C). There were no changes in liver weight (Fig. 4D).

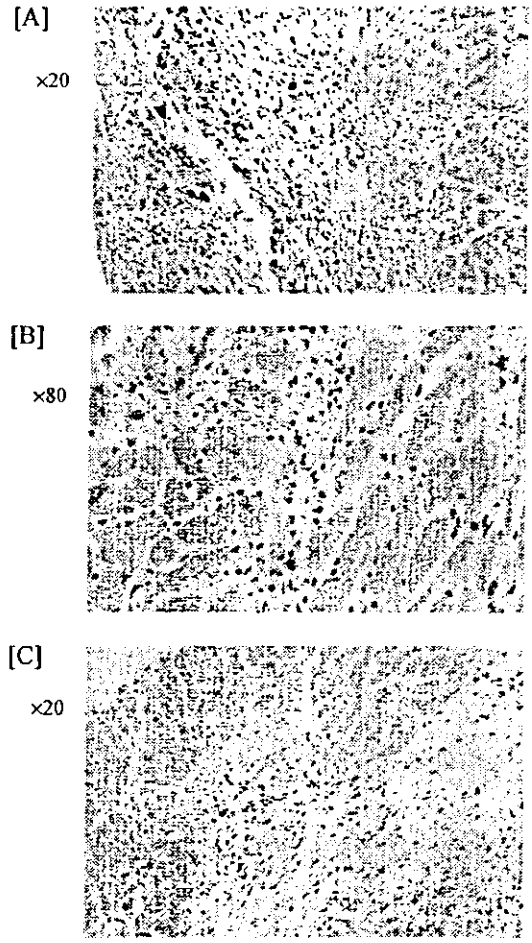

Figure 3. Histological analysis of dead DBA/2 mice administered with CAWS. [A, B, C] CAWS (4mg/mouse) was administered i.p. to DBA/2 mice for five consecutive days in the 1st and 5th week. Thereafter, the hearts of dead mice were stained with hematoxylin-eosin.

Cytokine Production by Spleen Cells of CAWS-Administered Mice on Stimulation with CAWS

As splenocyte counts in DBA/2 mice were high, we examined the production of cytokines in response to CAWS. Spleen cells of mice administered CAWS to induce coronary arteritis were prepared at a concentration of 1×10^7 cells/ml, and cultured for 48 hours in a 5% CO_2 incubator at 37° for observing cytokine production. Following the culture, IL-1β, IL-4, IL-6, IL-10, IL-12, IFN-α, and TNF-α levels in the culture supernatant were measured by ELISA. The strains with severe coronary arteritis, C3H/HeN, DBA/2 and C57BL/6 mice, showed IL-1β and IL-6 production by spleen cells in the CAWS -administered group (Fig. 5). In contrast, IL-10 was significantly produced

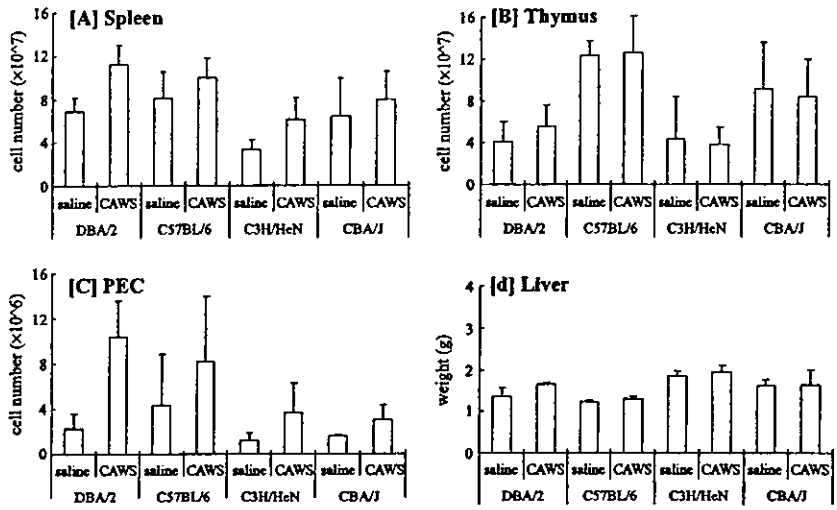

Figure 4. Cell number in peripheral blood and organ weight from CAWS-administered mice. CAWS (0 or 4mg/mouse) was administered i.p. to DBA/2, C57BL/6, C3H/HeN and CBA/J mice for five consecutive days in the 1st and 5th week. In the 9th week, the internal organs were collected from each mouse. Total cell number was counted with a hemocytometer and organ weight was measured with a analytical balance. The results show the mean ± standard deviation (S.D.). *; $P<0.05$ compared with the control using Student's *t-test*. [A]: Spleen, [B]: Thymus, [C]: PEC, [D]: Liver.

by spleen cells of the CBA/J mouse, which is the strain resistant to the coronary arteritis induced by CAWS.

In order to observe CAWS-specific reactions, the spleen cells of mice administered CAWS were stimulated with CAWS (0, 2.5, 5 or 10 μg/ml) and cultured for 48 hours in a 5% CO_2 incubator at 37°C. IFN-γ, IL-6 and IL-10 levels correlated well with the degree of coronary arteritis induced by CAWS (Fig. 6). IFN-γ and IL-6 production in DBA/2 and C57BL/6 mice tended to increase during the CAWS-specific response in the CAWS groups as compared with the saline groups, but no response was observed in C3H/HeN and CBA/J mice. IL-10 production was particularly enhanced in CBA/J mice treated with CAWS and slightly increased in the saline group, but no significant increase in production was observed even with the administration of CAWS in DBA/2 and C57BL/6 mice, and only a slight increase in C3H/HeN mice. Levels of other cytokines were not correlated with the coronary arteritis caused by CAWS. The amount of IL-4 production was small in all strains, but increased somewhat in CBA/J and C3H/HeN mice. IL-12 was hardly detected in any of the strains.

Measurement of Anti-CAWS Antibody Titer

Serum was obtained from mice administered CAWS in accordance with the coronary arteritis induction protocol, and anti-CAWS antibody in serum was detected with anti-mouse IgG + IgM Ab. Anti-CAWS antibodies were detected in all of the